13-17 July 2014, Tucson, Arizona

Compact Multi-gas Monitor for Life Support Systems Control in Space: Evaluation Under Realistic Environmental Conditions

Jesús Delgado Alonso[1] and Straun Phillips[2]
Intelligent Optical Systems, Inc., Torrance, CA, 90505

Cinda Chullen[3]
NASA Lyndon B. Johnson Space Center, Houston, TX, 77058

and

Edgar Mendoza[4]
Redondo Optics, Inc., Redondo Beach, CA, 90277

Advanced space life support systems require lightweight, low-power, durable sensors for monitoring critical gas components. A luminescence-based optical flow-through cell to monitor carbon dioxide, oxygen, and humidity has been developed and was demonstrated using bench-top instrumentation under environmental conditions relevant to portable life support systems, including initially pure oxygen atmosphere, temperature range from 50°F to 150°F, and humidity from dry to 100% RH and under conditions of water condensation. This paper presents the most recent progress in the development of this sensor technology. Trace gas contaminants in a space suit, originating from hardware and material off-gassing and crew member metabolism, are from many chemical families. The result is a gas mix much more complex than the pure oxygen fed into the space suit, and this complexity may interfere with gas sensor readings. This paper presents an evaluation of optical sensor performance when exposed to the most significant trace gases reported to be found in space suits. A study of the calibration stability of the sensors is also presented. For that purpose, a profile of temperature, pressure, humidity, and gas composition for the duration of an EVA has been defined, and the performance of sensors operated repeatedly under those conditions has been studied. Finally, this paper presents the first compact readout unit for these optical sensors, designed for the volume, power, and weight restrictions of a PLSS.

Nomenclature

τ	=	emission lifetime
EMI	=	electromagnetic interference
EMU	=	extravehicular mobility unit
EVA	=	extravehicular activity
FOCS	=	fiber optic chemical sensor
ISS	=	International Space Station
LED	=	light emitting diode
ϕ	=	phase
NDIR	=	Non-Dispersive Infrared
pCO_2	=	partial pressure of carbon dioxide
PLSS	=	Portable Life Support System

[1] Senior Scientist, and 2520 W. 237th Street, Torrance, CA 90505.
[2] Chemist, and 2520 W. 237th Street, Torrance, CA 90505.
[3] Project Engineer, Space Suit and Crew Survival Systems Branch/EC5, 2101 NASA Pkwy, Houston, TX 77058.
[4] CEO/President, and 811 Catalina Ave., Suite 1100, Redondo Beach, CA 90277.

pO_2 = partial pressure of oxygen
RH = relative humidity

SBIR = Small Business Innovation Research
SMAC = spacecraft maximum allowable concentration
Sn-1 = standard deviation
TC = trace contaminant

I. Introduction

FIBER optic chemical sensors (FOCS) based on luminescence includes a sensitive material, a light source, optical fibers, a photodetector, optical filters, analog amplifiers, and signal processing hardware and software. Light at a wavelength selected by an optical filter is launched into the core of the optical fiber. The fiber waveguide carries the excitation light to the probe tip, from which it shines on the sensing material containing an indicator dye inmobilized in a polymeric matrix, whose emission is affected by the presence of the analyte. The indicator is excited by the light, and returns the excess energy in the form of fluorescence (or luminescence). If there is a selective interaction with the target analyte species (O_2, CO_2, H_2O…), the luminescence of the sensing material undergoes a measurable change in intensity. Concomitantly, in the sensors we have developed for the PLSS, the emission lifetime (the time between absorption of excitation photons and emission of luminescent photons) is strongly affected. The modified light emitted by the sensing material is guided back through the optical fiber and a filter matching the emission wavelength to a photodetector. The resulting electrical signal is amplified and then digitized for processing.

The sensors we have developed for the PLSS measure emission lifetime, in contrast to amplitude measurements, making these measurements stable and reliable. The emission lifetime does not depend on the excitation source intensity or the detector response, and it is insensitive to movements of the optical fiber. Phase-resolved luminescence detection determines emission lifetime indirectly,[1] by means of compact and low-power electronics.

Luminescence-based fiber optic sensors performing phase-resolved measurements to monitor oxygen, carbon dioxide, humidity and temperature in Portable Life Support Systems have been developed and their characteristics determined by means of benchtop instrumentation, as reported previously.[2] Miniaturization and operation under liquid water condensation are some of the characteristics unique to these sensors. Further studies to evaluate the luminescence-based CO_2 sensors under potential environmental conditions in the PLSS are presented in this paper, including operation at reduced pressure, operation in the presence of trace contaminants, and stability through repeated operation for the length of an EVA.

Non-Dispersive Infrared (NDIR) sensing technology represents the current state-of-the-art for measuring CO_2, and today NDIR remains the most accurate, durable, long-term, and stable CO_2 monitoring technology for space systems. However, it is sensitive to the free water that can condense or accumulate in the gas sampling area, particularly on the optical windows, and it is this condensation that has historically been the cause of sensor failures. It is reported that 7% of EVA problems in the ISS resulting in mission aborts have been caused by CO_2 sensor failures. For this reason, the novel fiber optic sensors for carbon dioxide monitoring are of particular interest.

II. Evaluation of Calibration Stability

The stability of the calibration of the novel CO_2 sensors during repeated operation was studied. Operation of the CO_2 sensor at elevated temperature has been identified as the main factor that could cause sensor signal drift and eventually make recalibration necessary. Therefore, tests were designed to cycle the sensor material temperature between ambient and elevated during CO_2 response tests. The testing sequence including elevated temperature runs for eight hours, the length of an EVA, and is repeated ***n*** times (n >12) for each sensor material under evaluation. Performance at 25°C was taken as a benchmark to analyze sensor stability. The 25°C calibration curves (sensor signal vs. pCO_2) were recorded before and after each eight-hour run. Because the sensor system will only operate during EVA, sensor operation over a period of several years can be evaluated in just a few weeks.

Initially, sensor materails were tested at temperatures up to 50°C (four to six hours out of the eight-hour test); once the sensor stability was established under those conditions, the peak test temperature was raised to 66°C. Although the temperature range specified for the PLSS goes up to 66°C, exposure of the sensor for four hours at that temperature exceeds typical environmental conditions in an EVA, leaving a significant margin of safety in the sensor longevity determination. The calibration parameters of the sensor were evaluated in the 0 to 0.30 psi range, although some of the tests exposed the sensor to as much as 1.5 psi pCO_2. Table 1 records the temperature sequence of the tests. Test 1 exposed the sensor cyclically to increasing levels of CO_2 and to balance gas. These tests were

conducted at constant relative humidity (75% RH) and ambient pressure, with nitrogen or synthetic air as the balance gas. Tests at reduced pressure and variable humidity were conduced separately.

Table 1. Temperature sequence of sensor material testing.

	n Cycles. 1 hour Stabilization between T Steps			
Temperature / Time	8 hours		8 hours	
Temperature 2				Test 1
Temperature 1		Test 1		
25°C	Test 1		Test 1	

The setup for the tests is diagrammed in Figure 1. The sensor temperature is controlled by placing the probe in a flow cell in an Espec ECT-3 benchtop temperature chamber. Gas streams with controlled RH values are generated by volumetrically mixing saturated gas with dry gas. The flow of moist gas and dry gas is precisely controlled by programmable digital mass flow controllers. In this test, bubblers saturate the gas stream with water. While a dew point generator would more accurately control the moisture of the gas stream, the use of a bubbler is convenient when tests are conducted at varying temperatures. Being able to house both the sensor probe and the bubblers in the temperature chamber makes it easy to program tests around the clock, at varying temperatures and humidity levels.

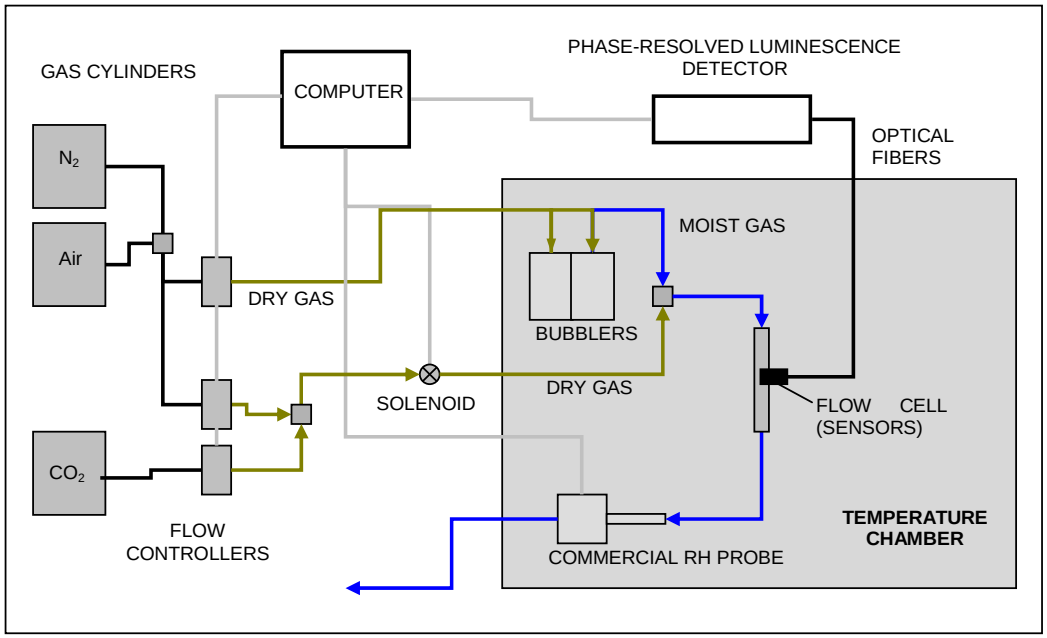

Figure 1. Typical configuration of the experimental setup for testing the sensors in a temperature chamber, with bubblers to saturate the air.

Because one objective of this study was to evaluate the potential of several sensor materials, we evaluated sensors prepared with a number of polymeric matrixes. Figure 2 shows the response profile (phase shift) of a typical sensitive film exposed to CO_2 cycling at varying temperatures during a typical test. As expected, the sensitivity of the sensor material declines as the temperature increases. In an actual CO_2 sensor device, a temperature correction will be applied to the raw sensor signal to compensate for this effect.

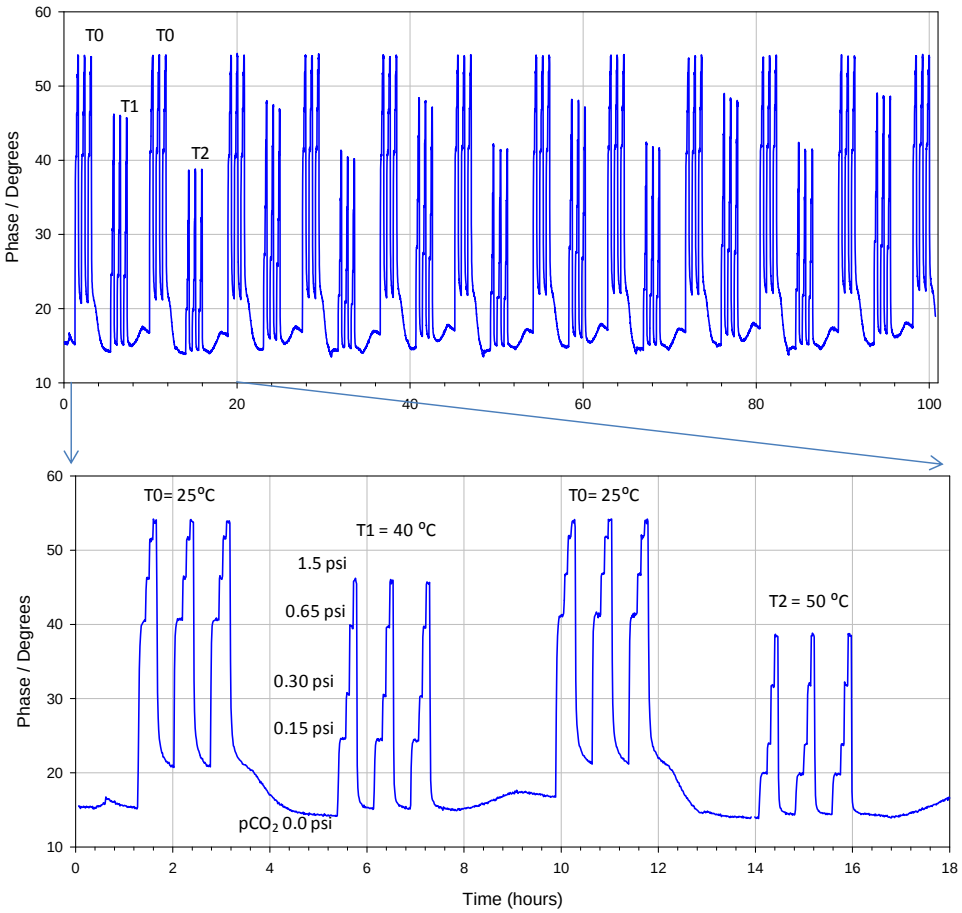

Figure 2. Top: Response profile of a CO_2 sensor material when exposed cyclically, at varying temperatures, to varying partial pressures of CO_2 in nitrogen. Bottom: Detail of the first 12 hours of testing.

The 25°C calibration curves (sensor signal vs. pCO_2) for each cycle, and the phase shift values for three CO_2 concentrations (0, 0.15 and 0.30 psi) recorded at 25°C during the tests were extracted and plotted for each sensor formulation evaluated. Figures 3 and 4 show the results observed for four sensor formulations.

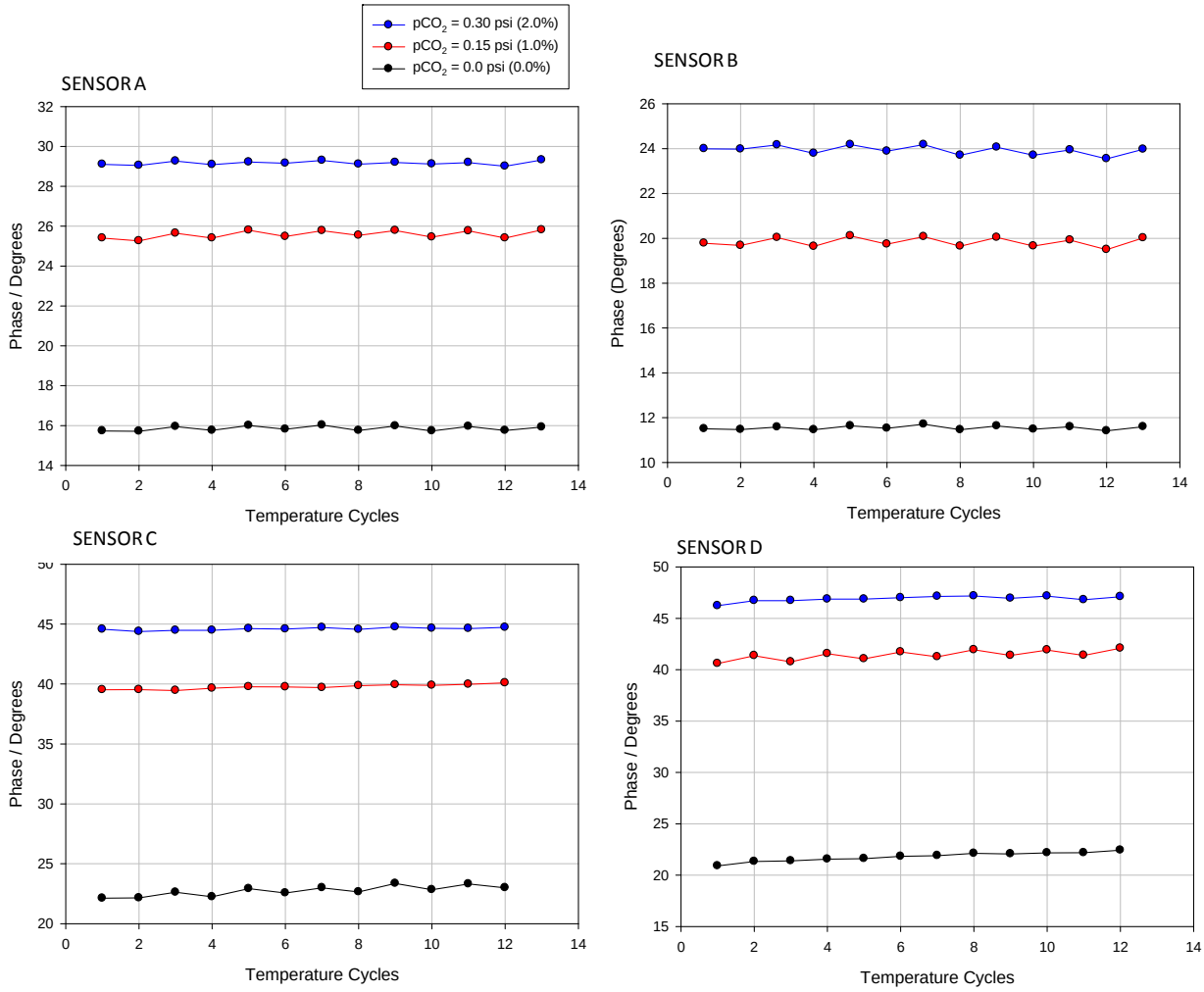

Figure 3. Stability curves: Phase shifts recorded at 25°C for four sensor materials at 0.0, 0.15, and 0.30 psi *p*CO_2 during a stability test conducted at up to 50°C.

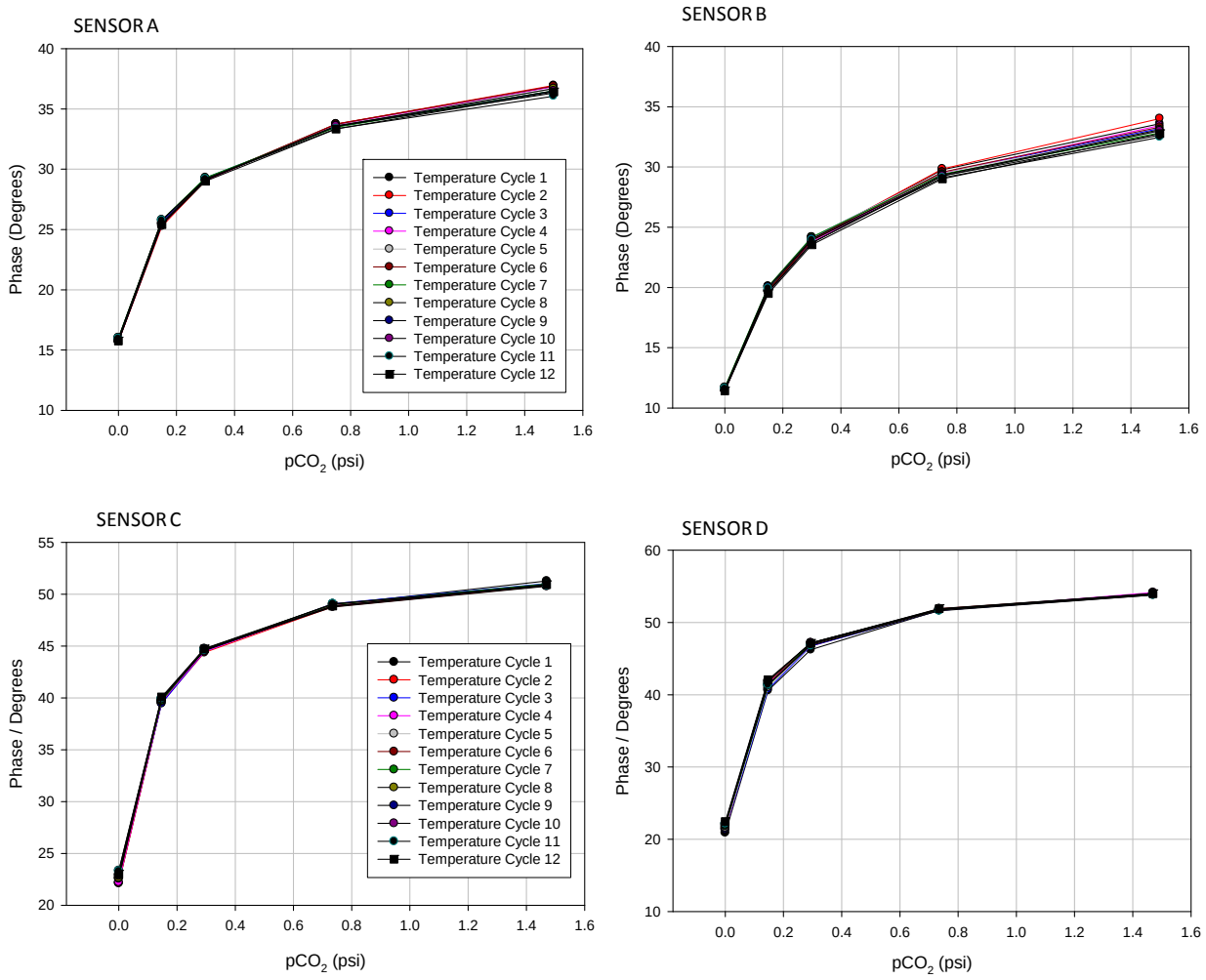

Figure 4. Calibration curve (phase vs. pCO_2) at 25°C for four sensor materials during a stability test conducted at up to 50°C.

Sensors C and D show behavior typical of sensor materials exhibiting good stability. Sensors A and B illustrate sensors with limited stability whose calibration curves change slightly during the test. The potential of the sensors to measure accurately through a number of EVAs was demonstrated in a test conducted at 50°C and at 66°C, so the temperature profile for the tests is more aggressive than a typical EVA temperature profile. Studies to determine the stability of the calibration parameters during storage have been designed and will be the focus of future work.

III. Tests at Reduced Pressure

Most of our tests designed to determine the sensor characteristics are conducted at ambient pressure, which simplifies the testing setup and facilitates operation under pure oxygen. It was assumed that the sensor characteristics at ambient and reduced pressures are the same or very similar. To confirm that assumption, the test setup was modified to operate the system at reduced pressure, simulating the environmental conditions found on the PLSS, as illustrated in Figure 5.

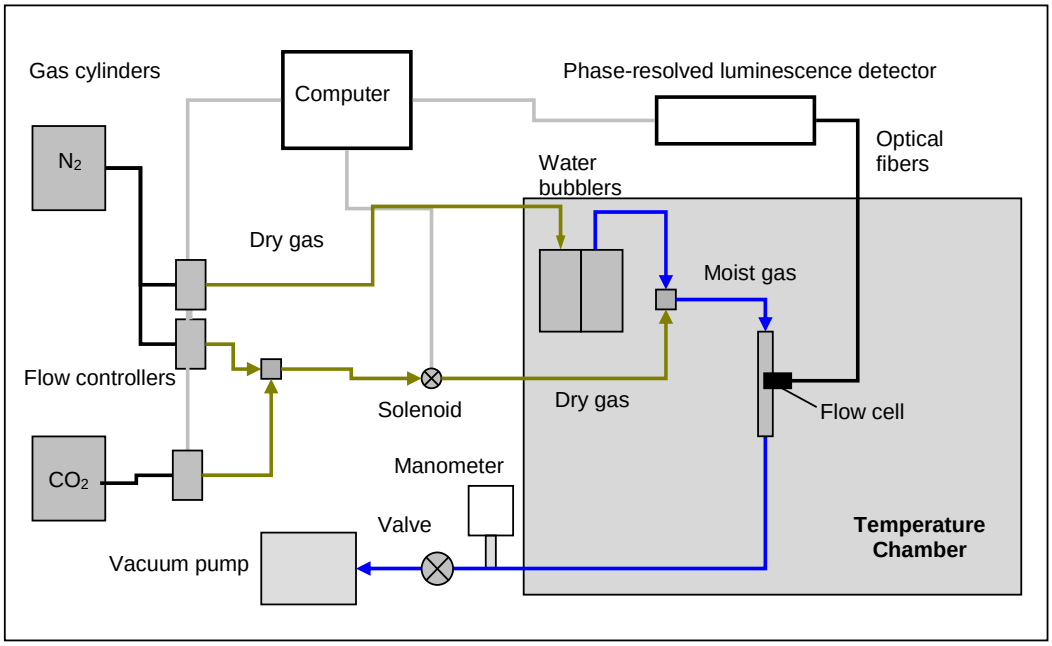

Figure 5. Typical configuration of the experimental setup for testing the sensors at reduced pressure.

An absolute pressure of 4.7 psi was selected for these tests. The first series of tests exposed the sensors to three values of pCO_2 at a total pressure of 4.7 psi, and to ambient pressure of 14.7 psi (Figure 6). As expected, sensor response is proportional to pCO_2 instead of to the molar fraction; therefore, the total pressure of the system does not affect the sensor signal for a particular pCO_2 (Figure 7). Thus, **sensor signal correction for pressure is not necessary, although it is requested in the majority of gas sensor systems**. This test was conducted at two humidity levels, maintaining the partial pressure of water constant through both tests.

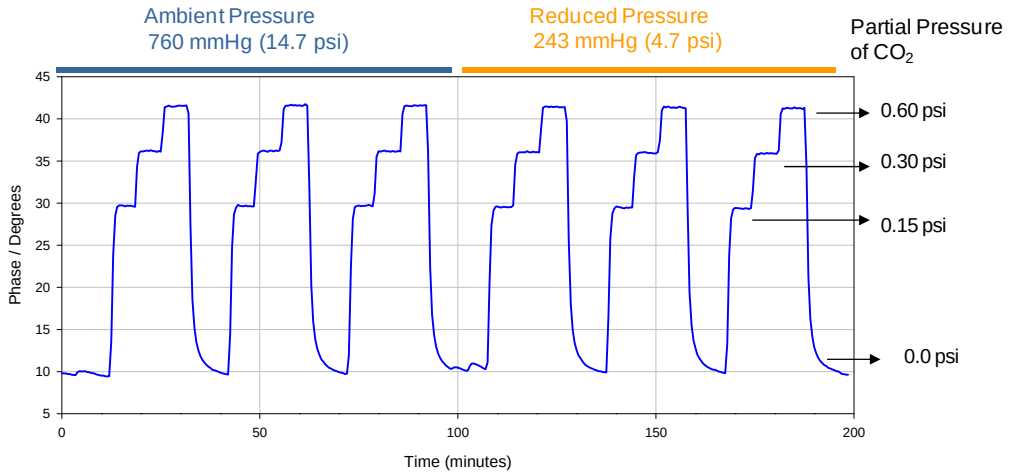

Figure 6. Response profile of a sensor material exposed to varying partial pressures of CO_2 in nitrogen at 14.7 psi and at 4.7 psi total pressure at 25°C, using dry gases.

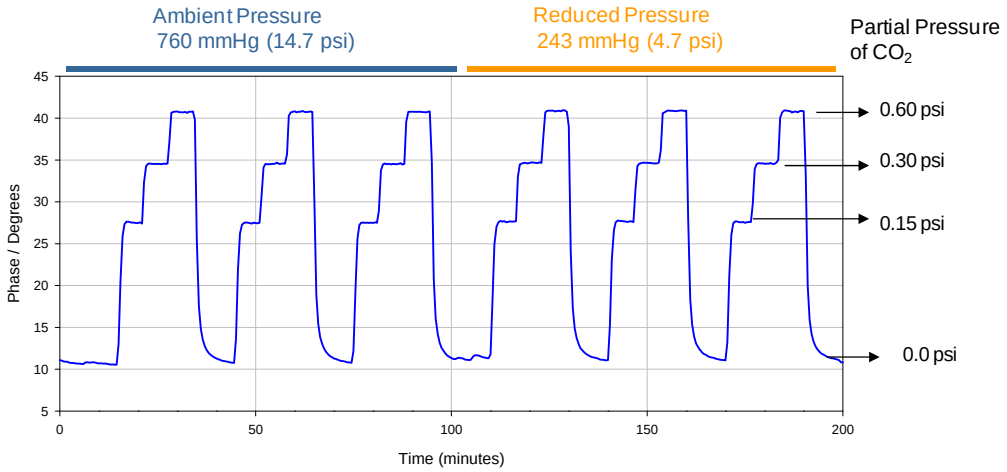

Figure 7. Response profile of a sensor material exposed to varying partial pressures of CO_2 in nitrogen at 14.7 psi and at 4.7 psi total pressure at 25°C and at pH_2O = 12.0 mmHg (50% RH @ 760 mmHg).

The second series of tests conducted at reduce pressure reproduced the sequence used for the calibration stability evaluation described above, usually at ambient pressure, 4.7 psi (Figure 8). **No differences in sensor stability were observed between testing at reduced pressure, and at ambient pressure**. The variability observed in the phase values in the tests does not exhibit a trend of steady increase or steady decrease, which are the fingerprints of sensor degradation, but rather can be related to variations in the experimental setup.

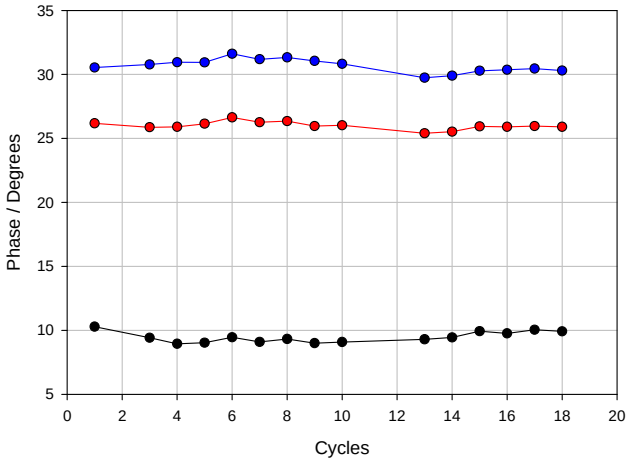

Figure 8. Phase shift recorded at 25°C at 0.0, 0.15 and 0.30 psi pCO_2, in a stability test conducted at up to 66°C and at 4.7 psi total pressure. Each cycle corresponds to eight hours of sensor operation.

IV. Sensor Evaluation in the Presence of Trace Contaminants

During EVA, trace contaminants (TC) produced by material, hardware, and crewmember off-gassing accumulate in the ventilation loop of the PLSS. The expected trace contaminants, generation rates, and spacecraft maximum allowed concentration, and the calculation of the concentration that could potentially be accumulated in the space suit, have been reported previously (Table 2).[3]

Table 2. Summary of expected constellation space suit PLSS ventilation loop trace contaminants, with generation rates,[4] spacecraft maximum allowable concentrations[5] and adverse effects.5

		Generation Rate	24-hr SMAC Limit		w/o Suit Leak
	Formula	*(mg/8-hr EVA)*	*(ppm)**	*(mg/m^3)*	**8-hr Concentration♦ (mg/m^3)**
Acetaldehyde**	CH_2CHO	0.027	6	10	0.181
Acetone	CH_3COCH_3	0.045	200	500	0.301
Ammonia	NH_3	83	20	14	564
n-Butanol	C_4H_9OH	0.017	25	80	1.13
Carbon monoxide***	CO	11	100	114	74.4
Ethyl alcohol	C_2H_5OH	1.3	5000	10000	9.03
Formaldehyde**	H_2CO	0.13	0.5	0.6	0.902
Furan	C_4H_4O	0.1	0.36	1	0.676
Hydrogen	H_2	17	4100	340	113
Methyl alcohol	CH_4	0.047	5300	3500	3.16
Methane	CH_3OH	200	70	90	1352
Toulene	C_7H_8	0.2	16	60	1.36

* Evaluated at 25°C and 1 atm
** Carcinogen
*** Carboxyhemoglobin target
♦ Shaded values exceed SMAC concentrations

The sensitive materials for CO_2 detection were initially exposed to a set of selected trace contaminants from Table 2 at up to the spacecraft maximum allowable concentrations (SMAC). The actual levels to be found in the space suit must be lower than the SMAC, so if the sensor is not affected by a particular gas at the SMAC level, we can assume that it will not be affected by that gas during an EVA. The tests were conducted with each of the inorganic gases on the list (ammonia, carbon monoxide, and hydrogen), and with methane and ethyl alcohol as examples of volatile organic compounds. These were selected because they represent the most adverse scenarios, since their SMAC levels are significantly higher than those for any other VOC. The behavior of the sensor in the presence of ethyl alcohol can be extrapolated for the presence of the other alcohols on the list, and lower reactivity should be expected for the aldehyde and ketone derivatives.

The sensors were tested at atmospheric pressure, 75% RH, 25°C, and with nitrogen as the balance gas, following the gas sequence plotted in Figure 9. In that way, the effect of each trace gas was evaluated over the CO_2 sensor base line (no CO_2%) and over the response of the sensor to CO_2 (at 1% CO_2: 0.15 psi).

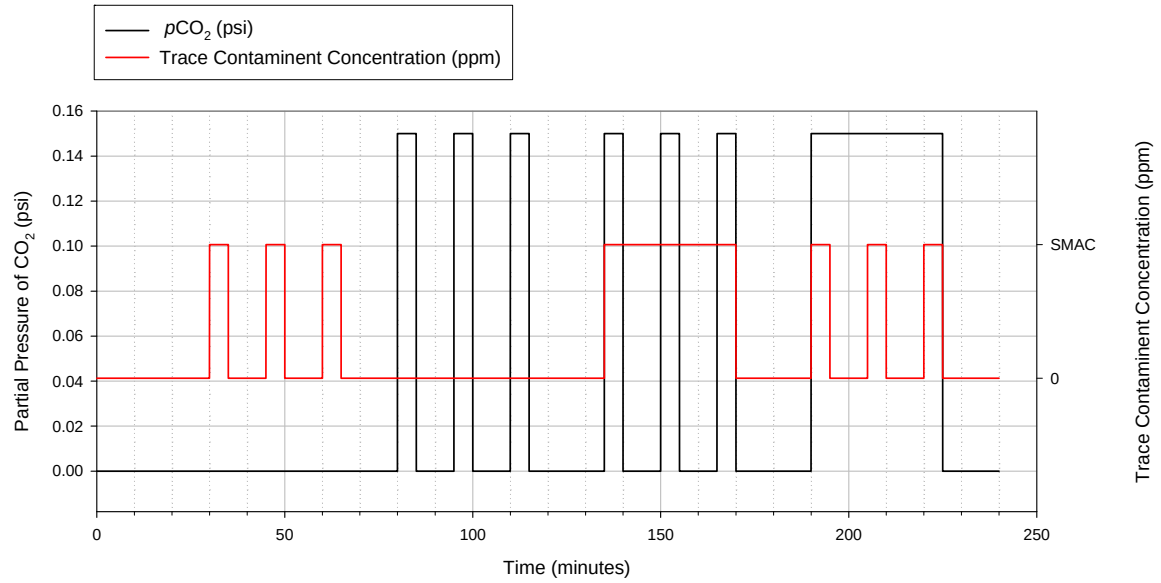

Figure 9. Gas sequence for evaluation of potential interference. SMAC: spacecraft maximum allowable concentration.

Figure 10 shows the response profile of a CO_2 sensor during the test conducted in the presence of hydrogen. Similar plots were recorded during the tests conducted in the presence of the selected trace contaminants.

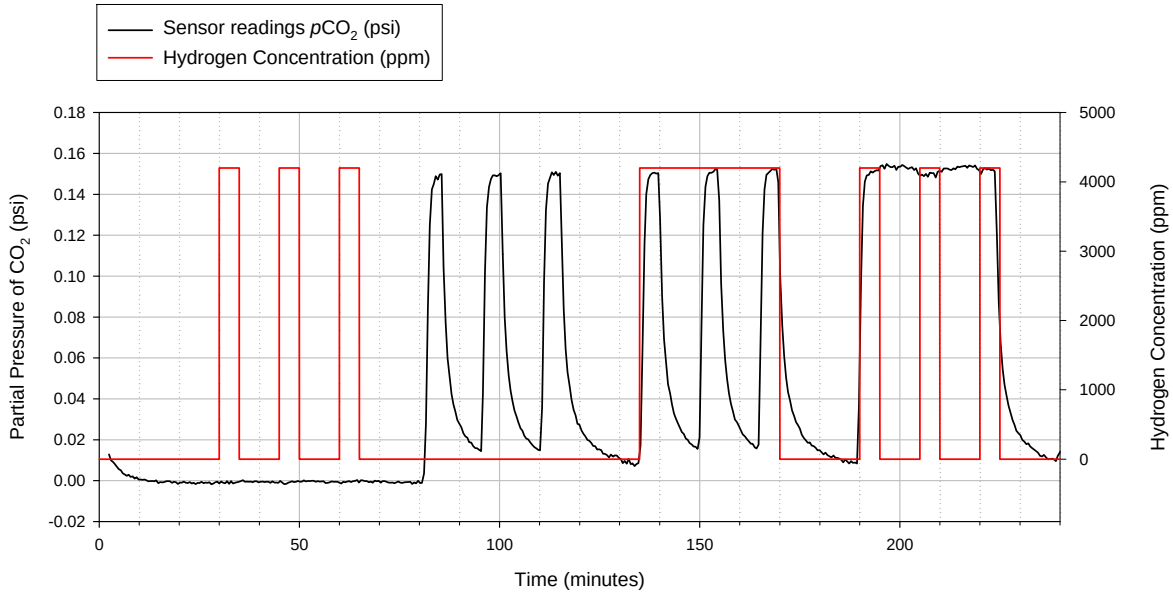

Figure 10. Response profile of a sensor material exposed to varying partial pressures of CO_2 in nitrogen (0 and 0.15 psi) in the presence of 4,200 ppm of hydrogen.

No significant effect on the sensor baseline or on the sensor response to CO_2 was observed in the tests conducted with ammonia, hydrogen, carbon dioxide, or methane at the spacecraft maximum allowable concentrations (see Table 3), so no further tests were conducted with these gases. However, the response of the sensor was affected by the presence of ethyl alcohol at 5,000 ppm, which is the SMAC for this VOC (Figure 11). Tests were then conducted at 1,000, 2,500, and 4,000 ppm and similar results were observed.

Table 3. Trace contaminant concentrations used for sensor evaluation and sensor readings (mean of ten data points) in the presence and absence of the trace contaminant.

TEST	Trace Contaminant	CO_2 Actual Partial Pressure (psi)	CO_2 Sensor Reading (psi)	Sn-1 (n=10)
Test 1	None	0.000	-0.001	< 0.001
	Hydrogen 4200 ppm	0.000	-0.001	0.001
	None	0.150	0.153	0.001
	Hydrogen 4200 ppm	0.150	0.150	0.001
Test 2	None	0.000	-0.002	< 0.001
	Methane 5600 ppm	0.000	-0.002	< 0.001
	None	0.150	0.149	0.001
	Methane 5600 ppm	0.150	0.151	0.001
Test 3	None	0.000	-0.003	< 0.001
	Carbon monoxide 100 ppm	0.000	-0.003	< 0.001
	None	0.150	0.149	0.001
	Carbon monoxide 100 ppm	0.150	0.147	0.001
Test 4	None	0.000	-0.005	< 0.001
	Ammonia 14 ppm	0.000	-0.005	< 0.001
	None	0.150	0.153	0.001
	Ammonia 14 ppm	0.150	0.152	0.001
Test 5	None	0.000	0.000	< 0.001
	Ethyl alcohol 45 ppm	0.000	0.001	0.001
	None	0.150	0.152	0.001
	Ethyl alcohol 45 ppm	0.150	0.154	0.001

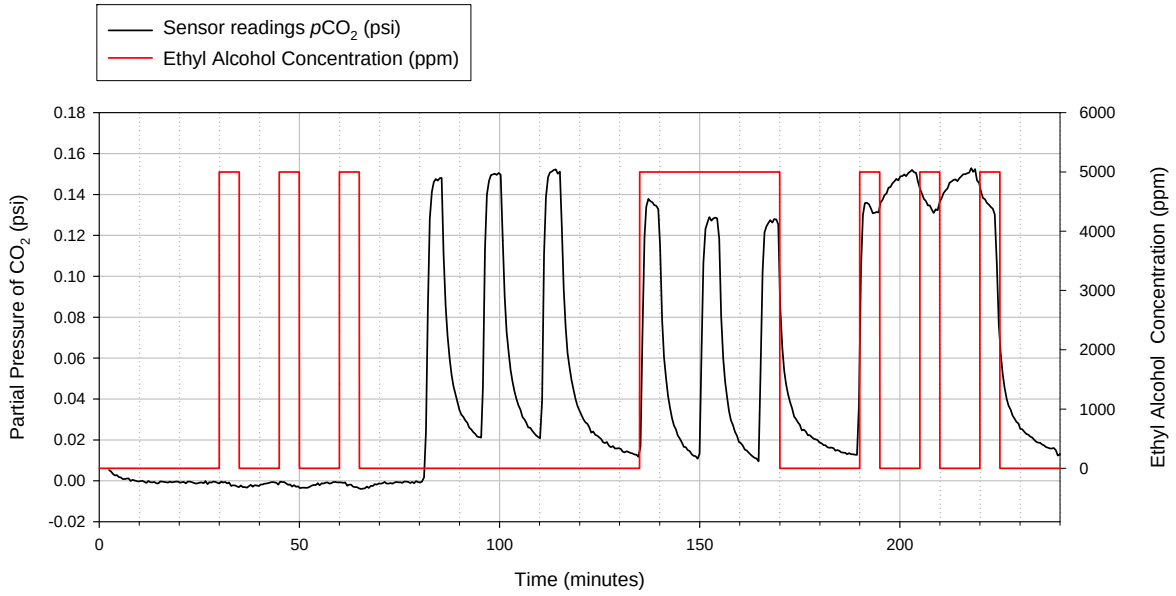

Figure 11. Response profile of a sensor material exposed to varying partial pressures of CO_2 in nitrogen (0 and 0.15 psi) in the presence of ethyl alcohol at 5,000 ppm.

The tests were therefore repeated at alcohol levels closer to concentrations that could be realistically found in the space suit. According to Table 2, the maximum concentration of ethyl alcohol that could be reached during a typical 8 hour EVA mission is only 4.5 ppm (in absence of a trace gas control system). The tests were repeated at 10 times that level (45 ppm) to assure proper sensor operation even in the most adverse scenario. No significant effect was

observed in the sensor baseline, nor in the sensor response to CO_2 during the test conducted at 45 ppm of ethyl alcohol (see Table 3).

V. Compact Readout Unit

Advances in sensor materials and the characterization of their analytical properties have been conducted in parallel to our development of the first version of a compact, low-power multichannel readout unit that can integrate four fiber optic sensors. An EMI-proof optical cable connects the remotely located readout unit to the flow-through cell containing the four sensitive materials for O_2, CO_2, and H_2O and temperature. For control of space systems, miniature fiber optic sensors connected to the electronic circuitry by an optical fiber cable allow greater flexibility in placing the sensor in highly constrained volume systems such as PLSS.

The readout unit is a phase-resolved luminescence detector module. In phase-resolved measurements, the instrument generates a continuous wave sinusoidal waveform of a known and programmable frequency that modulates the light source exciting the luminescent sensor materials. The emission intensity of the sensor materials is proportional to the excitation light intensity, and therefore is modulated at the same frequency as the excitation source. However, because the emission of photons by the excited molecules occurs some time after the absorption of energy, there is a delay between the excitation signal and the sensor signal. The instrument collects the sensor emission, and by comparison with the excitation signal determines the delay as phase shift (ϕ) between the two signals. An estimate of the fluorescence lifetime of the indicator probe can then be computed from the phase shift ($\tan\phi = 2\pi f\tau$), where f is the modulation frequency and τ is the emission lifetime of the probe.

This version of the electronic unit implements several strategies to increase flexibility and versatility during system development, but these will not be needed in the final product. Figure 12 is a block diagram of the system as it exists at present. The module for now communicates with a PC-based application for remote operation and data collection.

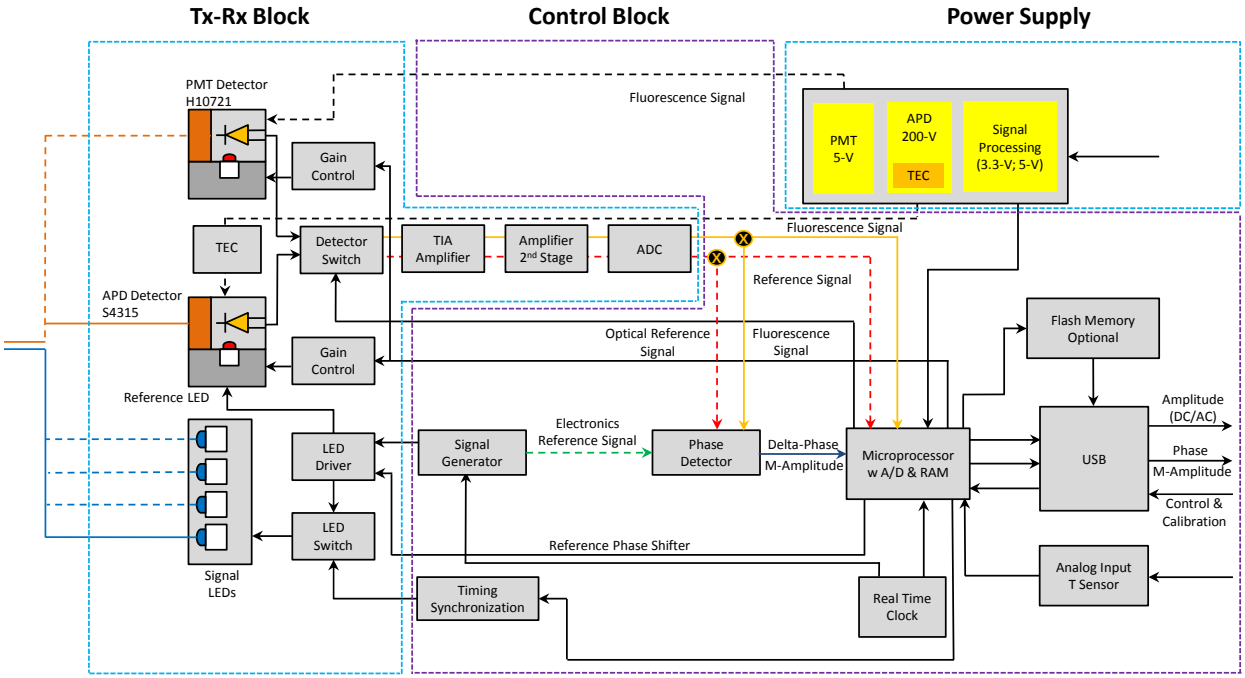

Figure 12. Basic block diagram of the phase-resolved luminescence detector module.

The two main blocks of the electronics unit are the Control Block and the Transmission – Reception block:

The main component of this digital block is a DSPIC33 microprocessor from Microchip's family of space qualified microcontrollers. This block performs six functions:

1. Calculate the operational parameters of the system, and program its components
2. Control the synchronization of the system, and generate the digital modulated signal
3. Determine the phase shift and amplitude of the emission
4. Perform system auto-diagnosis

5. Manage the user interfaces and communications
6. Determine the CO_2, O_2, and H_2O levels from the phase-shift and temperature measurements.

In this first version of the system, this module has been designed to explore two approaches to phase shift measurement (demodulation). The first (microprocessor-based phase detection) is conducted in the microprocessor. The second approach (demodulator-based phase detection) is based on a phase demodulator chip. This will enable us to evaluate the advantages and limitations of each, and to select one for the next system generation.

Since the relationship of phase shift to gas concentration is nonlinear, and since fluorescence lifetime depends on temperature (and, in the case of the CO_2 sensor, on humidity as well), further signal processing is required subsequent to the synchronous demodulation. Phase shift and temperature values (and humidity for the CO_2 sensor) must be compared to values in a three-dimensional or four-dimensional look-up table (including ϕ, temperature, RH, and gas concentration). The resulting gas concentration determination can be converted to a digital signal for interfacing with PLSS Caution and Warning System. This function is initially performed in the PC-user interface to facilitate sensor development, although it can also be implemented in the demodulation – linearization block without affecting any parallel functionality, since it requires simple mathematical data processing.

The transmission-reception block is an analog circuit that requires very little power and minimal space. The excitation components are a set of 470 nm LEDs coupled with multiplexed electronics. This block interfaces with the optical block.

Transmission: The modulated sequence of digital data generated in the demodulation block is converted into an analog sequence by a D/A converter with normalized levels of amplitude. The LED driver transforms these normalized levels into the required currents which, when applied to the light source, produce a light signal with the desired amplitude and frequencies. Additionally, a continuous current level is permanently applied to the LED to displace the work point and to ensure that at all times the device emits light in the zone of maximum linearity of its transfer function.

This block includes one blue LED for each sensor channel, and an additional red LED. The blue LEDs excite the luminescent signal of the sensor, and the red LED serves as a reference signal for determining phase shift. The reference signal, which does not interact with the sensitive material, enables the instrument to perform:

- Compensation for the delay introduced by the electronics in the original excitation signal, and for the temperature effects of the electronic circuitry
- Continuous auto-diagnosis. Phase-shift and amplitude calculation of two sequential periods of the reference signal can be used to continuously verify the proper operation of all the electronics, including all digital and analog blocks, and to warn of any error.

Reception: The reception block has a single photodetector to sequentially collect the signal from the four optical channels (sensors). An avalanche photodiode (APD) and a photomultiplier tube module (PMT) have been incorporated into the electronics unit, so we can evaluate the advantages and limitations of these two photodetection devices. The final design will incorporate only the photodetector that demonstrates the best overall signal-to-noise ratio, thermal stability, power consumption, size, robustness, etc.

The reception block is responsible for detecting the optical signal and amplifying the levels of the resulting electronic signal coming from the photodetector, for both the reference and the luminescent signal. It also carries out the next step of filtering the signal to maximize the signal-to-noise ratio, optimizing detection even under adverse conditions of stray light or external disturbances. This first version of the system incorporates a thermoelectric cooler and the associated driver for controlling the temperature of the APD.

Figure 13 shows the current version of the compact multichannel readout unit. The electronic unit has a volume of 250 cc and weight of 240 g. The power consumption measured with all the functionality operating simulataneously is 2.2 W, which establishes an maximum consumption level for this vrsion of the electronic unit.

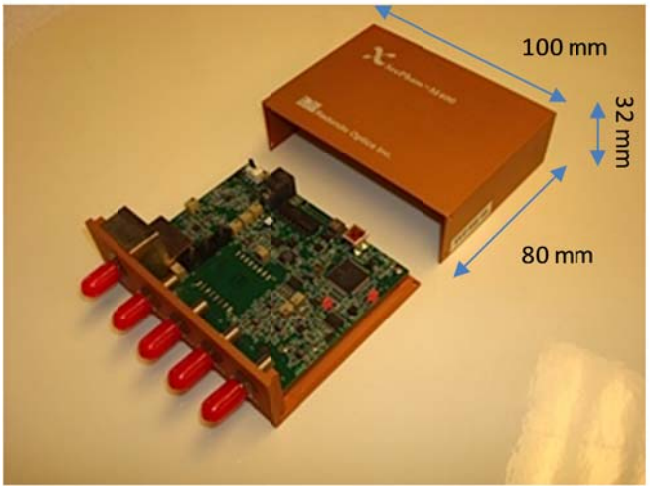

Figure 13. First prototype readout unit.

VI. Conclusions

The recent progress in the development of luminescence-based optical fiber sensors based on phase-resolved measurements for oxygen, carbon dioxide, humidity, and temperature monitoring in Portable Life Support Systems has been presented.

After documenting the device's capability of operating under conditions of liquid water condensation, and at temperatures ranging from 10°C to 65.5°C (50°F to 150°F), this paper has described the operation of the CO_2 sensors at reduced pressure, 4.7 psi. The sensor response to partial pressure of CO_2 does not depend on the total pressure of the system.

The stability of the calibration function of sensor materials for CO_2 has also been studied for several sensors, each fabricated with a different polymer.

The effect of the presence of trace contaminants found in space suits on the response of the CO_2 sensors has also been evaluated. No significant effect on the sensor baseline or on the sensor response to CO_2 was observed in the tests conducted with ammonia, hydrogen, carbon dioxide, methane, or ethyl alcohol at concentrations of at least 10 times higher than the maximum concentration expected in the space suit for each of them or at the spacecraft maximum allowable concentrations (SMAC).

The first compact readout unit for these optical sensors, designed for the volume, power, and weight restrictions of a PLSS, has been developed. The unit implements parallel strategies for performing the fundamental processes involved in sensor signal detection, phase shift calculation, and evaluation. The volume, weight, and power requirement of this first unit demonstrate the potential of this technology for implementation in constrained volume systems such as PLSS.

Acknowledgments

This research has been supported through the NASA SBIR program (Contract NNX11CE46P). The success of this work reflects the support received from Mr. Colin Campbell and Mr. Gregory Quinn.

References

[1]Holst, G. A., Kühl, M., Klimant, I., and Scheggi, A. V., "Novel Measuring System for Oxygen Micro-Optodes based on a Phase Modulation Technique," *Proceedings of SPIE - The International Society for Optical Engineering*, 2508, 1995, pp. 387-398.

[2]Delgado Alonso, J., and Chambers, A., "Miniature Sensor Probe for O_2, CO_2, and H_2O Monitoring in Portable Life Support Systems," *43rd International Conference on Environmental Systems*, 2013.

[3]Paul, H. L., and Jennings, M. A., "Requirements and Sizing Investigation for Constellation Space Suit Portable Life Support System Trace Contaminant Control," NASA Johnson Space Center, Glenn Waguespack, Geocontrol Systems, Inc., 2010.

[4]"Constellation Program Extravehicular (EVA) Systems Project Office (ESPO) Space Suit Element Requirements Document," CxP 72208, rev C.3, Houston: NASA/Johnson Space Center, September 22, 2009.

[5]"Spacecraft Maximum Allowable Concentrations for Airborne Contaminants," JSC-20584, Houston: NASA/Johnson Space Center, November 2008.